1   **Increased Primary and Secondary H₂SO₄ Showing the Opposing Roles in SOA**

2   **Formation from Ethyl Methacrylate Ozonolysis**

3   Peng Zhang [a, c,#], Tianzeng Chen [a, c,#], Jun Liu [a, c], Guangyan Xu [a, c], Qingxin Ma [a, b, c *],

4   Biwu Chu [a, b, c*], Wanqi Sun[d], and Hong He [a, b, c]

5   [a] State Key Joint Laboratory of Environment Simulation and Pollution Control,

6   Research Center for Eco-Environmental Sciences, Chinese Academy of Sciences,

7   Beijing 100085, China

8   [b] Center for Excellence in Regional Atmos. Environ., Institute of Urban Environment,

9   Chinese Academy of Sciences, Xiamen 361021, China

10   [c] University of Chinese Academy of Sciences, Beijing 100049, China

11   [d] CMA Meteorological Observation Centre, Beijing, 100081, China

12   [#] These authors contributed equally to this work

26

27

28

29

30

31

Abstract

Stressed plants and polymer production can emit many unsaturated volatile organic esters (UVOEs). However, secondary organic aerosol (SOA) formation of UVOEs remain unclear, especially under complex ambient conditions. In this study, we mainly investigated ethyl methacrylate (EM) ozonolysis. Results showed that a substantial increase in secondary H_2SO_4 particles promoted SOA formation with increasing SO_2. An important reason was that the homogeneous nucleation of more H_2SO_4 at high SO_2 level provided greater surface area and volume for SOA condensation. However, increased primary H_2SO_4 with seed acidity enhanced EM uptake, but reduced SOA formation. This was ascribed to the fact that the ozonolysis of more adsorbed EM was hampered with the formation of surface H_2SO_4 at higher particle acidity. Moreover, the increase in secondary H_2SO_4 particle via homogeneous nucleation favored to the oligomerization of oxidation products, whereas the increasing of primary H_2SO_4 with acidity in the presence of seed tended to promote the functionalization conversion products. This study indicated that the role of increased H_2SO_4 to EM-derived SOA maybe not the same under different ambient conditions, which helps to advance our understanding of the complicated roles of H_2SO_4 in the formation of EM-derived SOA.

49
50
51
52
53
54
55
56
57
58
59
60
61
62
63
64
65

66

67

1. Introduction

Unsaturated volatile organic esters (UVOEs) are oxygenated volatile organic compounds (OVOCs) with many large-scale commercial uses. They are not only used as potential replacements of traditional solvents and additive in diesel fuels but are widely used in the production of polymers and resins (Wang et al., 2010;Teruel et al., 2016;Blanco et al., 2014;Taccone et al., 2016;Colomer et al., 2013;Srivastava, 2009). Thus, the production, processing, storage, and disposal of industrial products all contribute to UVOE emissions. In addition, emissions of green leaf volatiles (GLVs), a class of wound-induced OVOCs, also contribute to UVOEs in the atmosphere (Hamilton et al., 2009;König et al., 1995;Arey et al., 1991). Once emitted into the atmosphere, these UVOEs quickly undergo complex chemical reactions with OH radicals and ozone in sunlight (Blanco et al., 2010;Bernard et al., 2010;Sun et al., 2015), NO_3 radicals during night-time (Wang et al., 2010;Salgado et al., 2011), and Cl atoms in certain environments (Blanco et al., 2010;Rivela et al., 2018). OH-initiated oxidation of GLVs, including *cis*-3-hexenylacetate (CHA) to secondary organic aerosol (SOA), is estimated to contribute 1–5 TgC/y, with up to a third of that from isoprene (Hamilton et al., 2009). In addition, CHA-derived SOA is a more efficient absorber (between 190 and 900 nm) than other OVOCs (such as *cis*-3-hexenol) due to the high proportion of carbonyl-containing species (Harvey et al., 2016). Thus, UVOEs can be considered as a class of potential SOA precursors. Further investigations on UVOE-derived SOA under complex ambient conditions will help to better understand their contribution to ambient aerosol.

Recent studies ascertained that the presence of SO_2 and sulfate seed particles all have a significant impact on the yield, composition, and formation mechanism of SOA (Zhang et al., 2019;Kristensen et al., 2014;Wong et al., 2015;Han et al., 2016). For example, an increase in SO_2 can enhance SOA production due to the formation of more sulfates and the enhanced acid-catalysis role during the atmospheric oxidation of various VOCs (Chu et al., 2016;Zhao et al., 2018;Lin et al., 2013). In the presence of

96   alone seed particles, however, increased particle acidity will not always enhance SOA

97   formation and may have a negligible effect on the SOA formation (Zhang et al.,

98   2019;Kristensen et al., 2014;Wong et al., 2015;Han et al., 2016;Surratt et al.,

99   2010;Eddingsaas et al., 2012;Riva et al., 2016). Furthermore, it is worth noting that

100   several studies have indicated that an increase in SO_2 can promote the average oxidation

101   state (OS_c) of SOA due to organosulfate formation (Zhang et al., 2019;Shu et al.,

102   2018;Liu et al., 2019a). whereas other studies have suggested that an increase SO_2 can

103   have a suppression effect on SOA OS_c (Friedman et al., 2016). Similarly, the effect of

104   increased aerosol acidity on SOA OS_c depends on the contribution of functionalization

105   and oligomerization reactions to SOA composition as increased aerosol acidity can

106   promote these reactions (Shu et al., 2018). This implies that the roles of increased

107   sulfate particles and particle acidity in SOA production and composition are very

108   complicated and need to be further studied.

109   Methacrylate was one of the main effluents in the class of UVOEs. Just in China,

110   the net import of methacrylate has up to about 930 thousand tons in 2019. It was worth

111   noting that ethyl methacrylate, one of methacrylate, has been widely detected in

112   ambient air due to the wide variety of sources and high volatility (Pankow et al., 2003).

113   Moreover, some exposure measurement studies indicated that the concentration of ethyl

114   methacrylate was up to 31-108 μg m^{-3} in the salons working air, which was notably

115   higher than other methacrylate (Henriks-Eckerman and Korva, 2012). Thus, we used

116   ethyl methacrylate (EM) as an UVOE proxy to investigate the effects of different SO_2

117   levels and seed particle acidity on the formation and evolution of EM-derived SOA in

118   this work. This work will help to better understanding the formation of EM-derived

119   SOA under complex conditions.

120

121   **2 Materials and methods**

122   Multiple EM ozonolysis experiments were conducted in a 30-m^3 cuboid Teflon smog

123   chamber (L × W × H = 3.0 × 2.5 × 4.0 m) under 298 K temperature and atmospheric

124   pressure. Experimental conditions are summarized in Table S1. The chamber operation,

125 analytical techniques, and experimental procedures are described in detail elsewhere

126 (Chen et al., 2019). Only a brief description on the specific procedures relevant to this

127 work is presented here.

128   Prior to each experiment, the smog chamber was cleaned for at least 24 h until

129 certain conditions were reached (i.e., <30 particle cm^{-3} and O_3, NOx, and SO_2

130 concentrations of <1 ppb). The O_3 (generated by passing 4 L min^{-1} dry zero air over two

131 UV photochemical tubes (40-cm length and 4-cm inter-diameter)), SO_2 (520 ppm in N_2,

132 Beijing Huayuan, China), and CO (0.05% in N_2, Beijing Huayuan, China) were added

133 into the chamber in sequence. EM were first added into a stainless-steel tee at 80 °C

134 and subsequently flushed into the chamber by zero gas with the flowrate of 20 L min^{-1}.

135 We applied CO to decrease the effect of OH radical reaction via scavenging of OH

136 radicals. The EM (98% purity, Sigma-Aldrich, USA) was added to the chamber by

137 injection of a known volume into a heated three-way tube (80 °C) and flushed into the

138 chamber by dry zero air. A fan made of stainless steel coated using Teflon was fixed at

139 the bottom of the chamber, which is used to ensure homogeneous mixing of reactants.

140   To minimize losses in the sampling line, various monitoring instruments

141 surrounded and are next to the smog chamber. The length of sampling pipes of various

142 monitoring instruments ranged from 0.5-1.0 m. A scanning mobility particle sizer

143 (SMPS, TSI, Inc.), consisting of a nano-differential mobility analyzer (DMA; model

144 3082), condensation particle counter (CPC; model 1720), and Po210 bipolar neutralizer,

145 was applied to measure number size distribution. Total particle number and mass

146 concentrations were calculated assuming a uniform density for aerosol particles of 1.4

147 g cm^{-3} (Liu et al., 2019b;Chen et al., 2019). The sheath flow and aerosol flow in the

148 SMPS were set to 3.0 and 0.3 L min^{-1}, respectively. The SMPS results were further

149 corrected via the wall loss rate of $(NH_4)_2SO_4$ particles and the correction magnitude is

150 about 10% in 5 h-reaction (Figure S1). Based on the different characterized fragments,

151 both mass concentration and evolution of the different chemical compositions of

152 aerosol particles were simultaneously measured online using High-Resolution Time-

153 of-Flight Aerosol Mass Spectrometric Analysis (HR-ToF-AMS; Aerodyne Research

154   Inc., USA). The AMS working principles and modes of operation are explained in detail

155   elsewhere. According to standard protocols, the inlet flow rate, ionization efficiency

156   (IE), and particle sizing were calibrated using size-selected pure ammonium nitrate (AN)

157   particles (Drewnick et al., 2005). The HR-ToF-AMS analysis toolkit SQUIRREL

158   1.57I/PIKA v1.16I in Igor Pro v6.37 was employed to process and analyze the

159   experimental data obtained by the HR-ToF-AMS. To reduce the sampling errors

160   resulting from calibrating HR-TOF-AMS before each experiment, the HR-ToF-AMS

161   results were further corrected using mass concentration derived from the SMPS as per

162   Gordon et al (Gordon et al., 2014). A series of gas analyzers from Thermo Scientific

163   (USA) were used to monitor the evolution of SO_2 (model 43i), CO (model 48i), and O_3

164   (model 49i) concentrations as a function of reaction time. Moreover, to make sure

165   results reliable and rule out potential artifacts including the adding sequence of CO, O_3,

166   and SO_2 during experimental preparation and the injection process of EM, parallel

167   experiments (twice experiments at the same experimental conditions) under selected

168   experimental conditions (135 ppb SO_2 and in the presence of AS seeds, respectively)

169   were conducted (Figure S2 and S3).

170

171   **3. Results and discussion**

172   **3.1. Overview of EM-derived SOA Formation with and without Seed Particles**

173   We first investigated the ozonolysis of alone EM. As shown in Figure S4, the

174   ozonolysis of alone EM could not produce SOA in the absence of seed and SO_2.

175   Similarly, the increased particle acidity did not promote SOA formation during the

176   ozonolysis of alone EM in the absence of SO_2 (Figure S5). Thus, this study mainly

177   focused on EM ozonolysis in the presence of SO_2. Secondary particle formation from

178   EM ozonolysis with different SO_2 levels was first investigated in the absence of seed

179   particles. As shown in Figure 1, SOA and sulfate were significantly produced once EM

180   was introduced into the reaction chamber. Moreover, both SOA and sulfate formation

181   were markedly enhanced with the increase in initial SO_2 concentration (Figure 1A and

182   B). This indicated that EM-derived SOA formation was closely related to sulfate

183   formation compared with that the ozonolysis of alone EM. Subsequently, EM

184   ozonolysis with the same level of SO_2 was also conducted in the presence of seed

185   particles with different acidity (neutral and acidic). Two different solutions, including

186   AS (0.02 mol L^{-1}) and AS + H_2SO_4 (0.02 + 0.04 mol L^{-1}), were nebulized into the

187   chamber, respectively, to provide the corresponding seed aerosol for acidity

188   experiments. The initial seed concentrations have been added in the Table S1.

189   Interestingly, with the increase of seed acidity, the maximum mass concentrations of

190   SOA and sulfate decreased from 19.1 to 12.9 $\mu g\ m^{-3}$ (Figure 1C) and 192.6 to 169.7 μg

191   m^{-3} (Figure 1D), respectively. This indicated that increased particle acidity suppressed

192   secondary particle formation in the presence of SO_2, which was inconsistent with the

193   enhancement effect of particle acidity via acid-catalysis on SOA formation during

194   alkene photooxidation (such as isoprene, isoprene epoxydiols, and glyoxal) (Kristensen

195   et al., 2014;Lin et al., 2011;Riva et al., 2016;Wong et al., 2015). In order to evaluate

196   whether the effect is atmospherically relevant, these experiments of seed particle role

197   were also conducted at higher RH (45-50% RH). As shown in Figure S6, it could be

198   found that increased particle acidity also suppressed the formation of SOA and sulfate

199   at higher RH. Moreover, the lower the concentration of both SOA and sulfate at 45%

200   RH relative to 10% RH proved that increased RH was adverse to SOA and sulfate

201   formation (Figure S7).Thus, these results imply that the increase of primary H_2SO_4

202   proportion with particle acidity in seed particles and the increase of secondary H_2SO_4

203   particles with SO_2 concentration exhibited the opposite role in EM-derived SOA

204   formation.

205
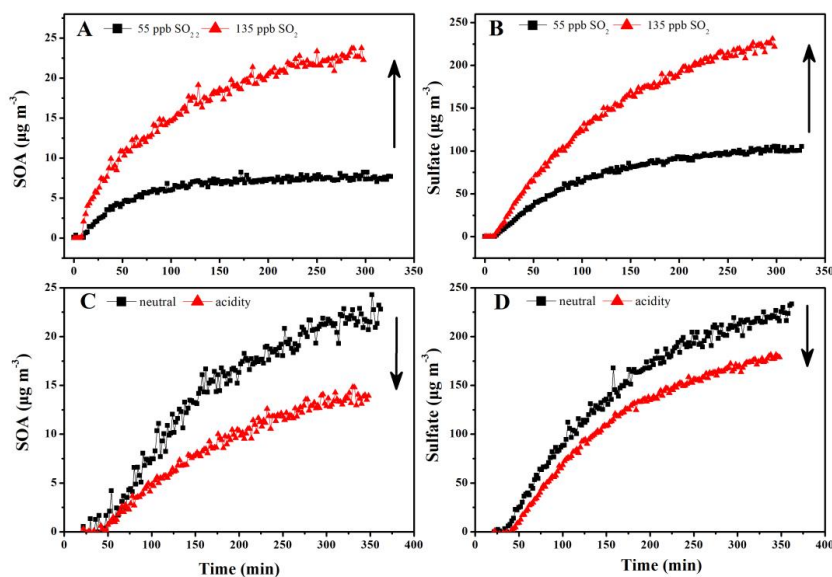
Figure 1. Time-dependent growth curves of SOA (A) and sulfate (B) under different

initial concentrations of SO$_2$ in absence of seed particles; SOA (C) and sulfate (D) after

subtracting seeds in presence of neutral and acidic seed particles.

As shown in Figure 2, the size distributions of secondary particles under different

experimental conditions were also compared. The detected maximum particle

concentration (790 000 particle cm^{-3}) under 135 ppb SO$_2$ was higher than that observed

under 55 ppb SO$_2$ (300 000 particle cm^{-3}) in the absence of seed particles (Figure 2A

and B). Recent studies suggested that the reaction between SO$_2$ and stable Criegee

intermediates (sCI) dominated the formation of H$_2$SO$_4$ particles and was enhanced with

increased SO$_2$ concentration. An important reason for this is the rapid homogeneous

nucleation of H$_2$SO$_4$ not only can provide greater surface area and volume for the

condensation of low-volatile products, but reduce the fraction of these semi-volatile

species lost to the wall (Zhang et al., 2019;Chu et al., 2016;Liu et al., 2017;Zhang et al.,

2014). In the presence of seed particles, we used similar average concentration

(~25 000-30000 particles cm^{-3}) and mode diameter (45 nm) of seed particles under

different acidities to reduce the disturbance of seed particle concentration (Figure 2C

and 2D). Results showed ~300 000 newly produced particles cm^{-3} for neutral AS seeds

(Figure 2C) and ~74 000 newly produced particles cm^{-3} for acidified AS seeds (Figure

224   2D), respectively. The reduction of NPF in the presence of acidic particles most likely

225   result from that acidic seed particles promoted the condensation of gaseous nucleation

226   species onto seed surface. However, this could not explain why both SOA and sulfate

227   were all suppressed with the increase in particle acidity. Thus, one reasonable

228   explanation is that acidic seed particles also enhanced EM uptake on the particle surface

229   as well as promoting the condensation of nucleation species. As a result, the

230   heterogeneous formation of fresher H_2SO_4 on the surface of seed particles subsequently

231   reduced SOA formation by hampering the ozonolysis of absorbed EM. To further

232   supported this speculation, the experiments on EM uptake and degradation on different

233   acidic seed particle were also checked using Fourier spectra and Mass spectrum

234   instruments. Result indicated that higher particle acidity indeed promoted EM uptake

235   on the particle surface and the presence of SO_2 resulted in the residual of more adsorbed

236   EM on particle surface (Figure S8 and S9).

237   In addition, as shown in Figure S5, the negligible change of SOA with acidity in

238   the absence of SO_2 also supported that the reducing effect of increasing particle acidity

239   on secondary particle formation was closely related to the formation of H_2SO_4 particles

240   in the presence of SO_2. And   some recent studies proved that some surface secondary

241   reactions involved Sci (Wang et al., 2016;Hearn et al., 2005), thus we couldn't

242   completely exclude the possibility that the suppressing role is likely related to the role

243   of increased acidity to sCI lifetime, which needed to be further explored in the future.

244   Moreover, the ozonolysis experiments of α-pinene at 45% RH in the presence of SO_2

245   with seed particles of different acidity were also carried out. Experimental results

246   indicated that increased particle acidity also suppressed the formation of both SOA and

247   sulfate during α-pinene ozonolysis at higher RH (Figure S10). This indicated the

248   reducing effect of increasing particle acidity to secondary particle in the presence of

249   SO_2 also could happen for other systems. Taken together, these results imply that the

250   SOA formation under different SO_2 levels and different particle acidities may be closely

251   related to the homogeneous or heterogeneous formation of H_2SO_4.

252
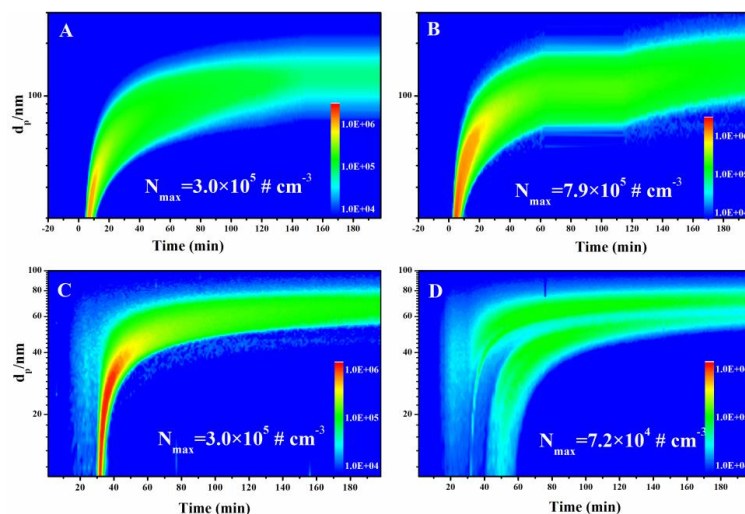
Figure 2. Size distribution of secondary aerosol as a function of time at 55 ppb SO_2 (A) and 135 ppb SO_2 (B) and under AS seed particle (C) and Acidic AAS seed particle (D).

255

3.2. Chemical Interpretation and Elemental Analysis of SOA

Recent studies have suggested that a higher proportion of H_2SO_4 in aerosol can result in greater formation of oligomers and high-oxygenated organic aerosol via acceleration of the acid-catalysis process (Zhang et al., 2019;Liu et al., 2019a;Shu et al., 2018). In order to make clear whether the homogeneous or heterogeneous formation of H_2SO_4 could also affect SOA composition. we further analyze SOA composition and evolution based on positive matrix factorization (PMF) solution and Van Krevelen diagrams (Zhang et al., 2005;Heald et al., 2010). The methodological of PMF analysis has been put into Supporting Information (Figure S11 and S12). The time series and mass spectra of each Factor after PMF analysis were applied to characterize the factor constitution and chemical conversion among factors (Ulbrich et al., 2009;Zhang et al., 2011).

Positive matrix factorization (PMF) solution

In the absence of seed particles, two factors were identified under different SO_2 concentrations. As shown in Figure 3A, the 43 ($C_2H_3O^+$) higher signals (tracers for alcohols and aldehydes) and prominent fragmental peaks containing one-oxygen atom

272   (i.e., C_2H_4O, C_2H_5O, C_3H_5O, C_3H_5O, C_3H_7O, C_4HO, and $C_6H_{10}O$) observed in Factor

273   1 implied that Factor 1 consisted of less-oxygenated organic aerosols. The 44 (CO_2^+)

274   higher signals, tracers for organic acids, and dominant peaks containing multi-oxygen

275   atoms (i.e., $C_3H_8O_3$, $C_3H_9O_3$, and $C_4H_{10}O_3$) observed in Factor 2 implied that Factor 2

276   consisted of more-oxygenated organic aerosols. From the temporal variations in Figure

277   3B, both Factor 1 and 2 continuously increased with reaction progress before 200 min,

278   implying that both factors were simultaneously produced during EM ozonolysis. After

279   200 min, Factor 1 continuously increased but Factor 2 decreased, suggesting that the

280   chemical conversion of part of less-oxygenated species in Factor 2 to more-oxygenated

281   products in Factor 1 in the latter period of reaction. Moreover, the average elemental

282   compositions of Factor 1 and Factor 2 were estimated to be $C_{2.29}H_3O_{0.53}S_{0.01}$ and

283    $C_{1.38}H_{1.87}O_{0.37}S_{0.027}$, respectively. Higher OS_c of Factor 2 (-0.81) relative to that Factor

284   1 (-0.85) also supported above conclusion. This also implied that the chemical

285   conversion from Factor 2 to Factor 1 could occur only when the H_2SO_4 proportion

286   (acidity) in the particle-phase reached a certain concentration (Offenberg et al.,

287   2009;Liu et al., 2019a). As shown in Figure 3C, the maximum production of both Factor

288   1 and Factor 2 increased with increasing SO_2. One reasonable explanation is that the

289   formation of more H_2SO_4 particles with increasing SO_2 provided a greater surface area

290   and volume for the simultaneous condensation of both less-oxygenated and more-

291   oxygenated organic products (Zhang et al., 2019;Chu et al., 2016;Liu et al., 2017). This

292   also indicated that the chemical conversion between the two factors could be ignored

293   in the absence of seed particles.

294
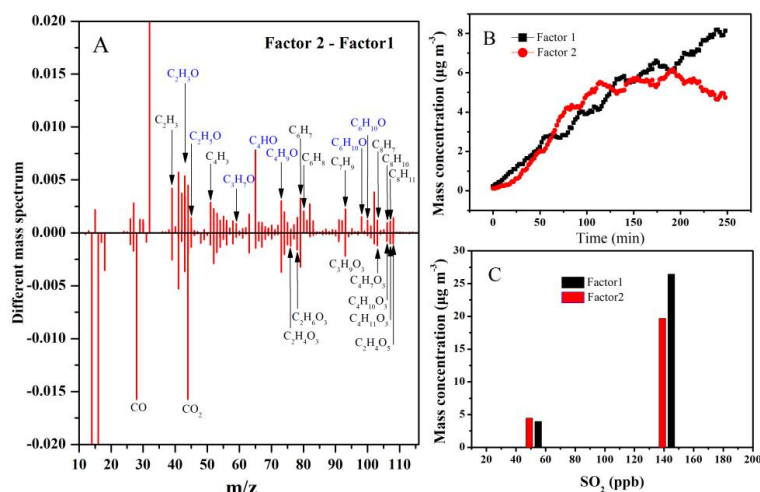
Figure 3. Two-factor solutions for PMF analyses of SOA under different SO_2 concentrations: (A) Different mass spectra between two factors (Factor 2-Factor 1) at 135 ppb SO_2; (B) Time series of factor concentrations; (C) Maximum concentration of two factors at 55 ppb and 135 ppb SO_2.

In the presence of seed particles, the chemical evolution of SOA components under different acidity conditions was also compared based on PMF analysis. From the temporal variations in Figure 4A, three factors were identified and almost simultaneously increased. Based on the mass spectra of the three factors (Figure 4B), the fragments containing less-oxygenated species in Factor 1 (such as typical fragment $C_2H_3O^+$ (m/z 43)) were more abundant than in Factor 2. In contrast, the fragments containing more-oxygenated species in Factor 2 (such as typical fragment CO_2^+ (m/z 44)) were more abundant than in Factor 1. Thus, Factor 1 and 2 were tentatively assigned to less-oxygenated and more-oxygenated organic aerosols, respectively. This proved that the increase in particle acidity simultaneously promoted the formation of both less and more-oxygenated species, similar to that in the SO_2 experiments. However, it is worth noting that higher acidity significantly promoted the chemical conversion of less-oxygenated species (Factor 1) to more-oxygenated species (Factor 2) via functionalization based on the comparison between the neutral and acidic seed particles (Figure 4C). As shown in Figure 4B, the ion at m/z 114 ($C_6H_{10}O_2$) was assigned to

314 precursor-related ions. The highest ion signal fraction (m/z 114) in Factor 3 and the

315 similar mass spectrum between EM and Factor 3 in Figure S13 implied that Factor 3

316 represented precursor-related species (Figure 4C).

317   Based on the comparison of Factors between seed experiments and SO_2, it should

318 be noted that Factor 1 and Factor 2 in the seed experiments differed from that in the

319 SO_2 experiment. For SO_2 experiments, acidity appeared to convert Factor 2 to Factor

320 1after 200 minutes, but in seed experiments, the more H_2SO_4 caused the formation of

321 more Factor 2 and less Factor 1. Thus, we concluded that, for the same Factor in two

322 types of experiments, the corresponding composition should be different each other.

323 One possible explanation for this was that the increase in primary and secondary H_2SO_4

324 particles could also affect SOA composition to some extent, such as via changing the

325 reaction pathway of sCI.
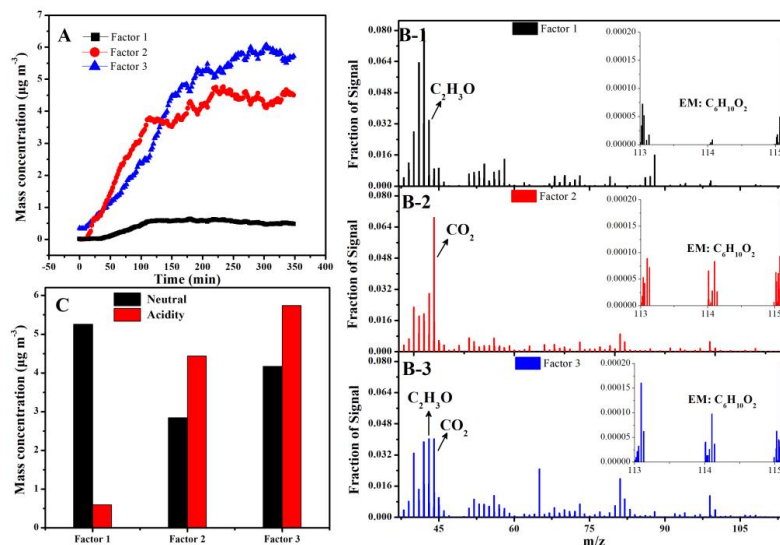
326

327 **Figure 4.** Three-factor solutions for PMF analyses of SOA under different seed

328 particles: (A) Time series of factor concentrations under acidic AAS; (B) Mass spectra

329 of three factors; (C) Comparison of maximum concentration of two factors under

330 neutral AS (black) and acidic AAS (red).

331 ***Elemental analysis in Van Krevelen diagrams***

332   The rate at which the H/C ratio changes with the O/C ratio in Van Krevelen

333 diagrams can provide new information about the functional groups formed during

334 oxidation (Lambe et al., 2012;Lambe et al., 2011;Li et al., 2019;Chen et al., 2011). As

335 shown in Figure 5A and 6A, the average (H/C)/(O/C) slopes under different

336 experimental conditions all approached -2. A slope of -2 is due to the formation of

337 carbonyl species (Ng et al., 2011). This is consistent with the acknowledged reaction

338 mechanism of alkene ozonolysis in the presence of SO_2, in which many carbonyl

339 species and H_2SO_4 particles are produced.(Sadezky et al., 2006;Sadezky et al.,

340 2008;Newland et al., 2015a;Newland et al., 2015b) To verify whether increased OS_c

341 was related to particle pH, particle pH was estimated using the E-AIM model (Model

342 II: $H^+ - NH_4^+ - SO_4^{2-} - NO_3^- - H_2O$) when secondary particle formation peaked under

343 different SO_2 concentrations (Peng et al., 2019;Hennigan et al., 2015). Since no

344 organics are considered in Model II, there was an inherent assumption here that the

345 acidity and the water uptake was dominated by the inorganic ions. From Figure 5B, it

346 could be found that the averaged oxidation state (OS_c) of SOA increased with

347 decreasing particulate pH in the absence of seeds. Similar trend was also observed in

348 the presence of seed particles (Figure 6B). This indicated that increased OS_c was closely

349 related to increased particles acidity either in the presence or absence of seed particles.

350 These results also indicated that both functionalization and oligomerization associated

351 with carbonyls groups dominate the formation of EM-derived SOA. Moreover, it is

352 worth noting that O/C increased when H/C decreased with increased particle acidity in

353 the absence of seed particles. In contrast, the O/C ratio increased but the H/C ratio

354 basically remained stable with increased particle acidity in the presence of seed

355 particles. These result implied that increased particle acidity tended to promote the

356 formation of more highly oxidized products via oligomerization in the absence of seed

357 particles and tended to promote the formation of more highly oxidized products via

358 functionalization in the presence of seed particles (Darer et al., 2011;Zhang et al.,

359 2019;Shu et al., 2018). However, the promoting contribution of SOA functionalization

360 conversion of total SOA could be ignored compared with the reducing effect of acidic

361 particles. Some studies showed that increased OS_c was closely related to the formation

362   of organosulfate (Zhang et al., 2019;Liu et al., 2019a;Shu et al., 2018). However, the

363   similar S/C ratio and sulfate fragments distribution between neutral and acidic seed

364   experiments excluded the contribution of organosulfate formation to increased OS_c

365   (Figure S14).

366

367
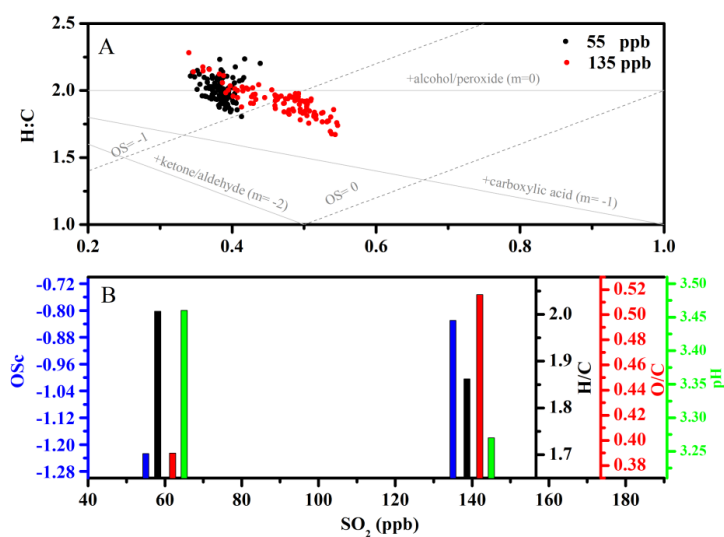
Figure 5. Van Krevelen diagrams of elemental ratios under different initial

concentrations of SO_2 (A); change in H/C ratio (black), O/C ratio (red), OS_c (blue), and

particle pH (green) as a function of initial SO_2 concentration (B).
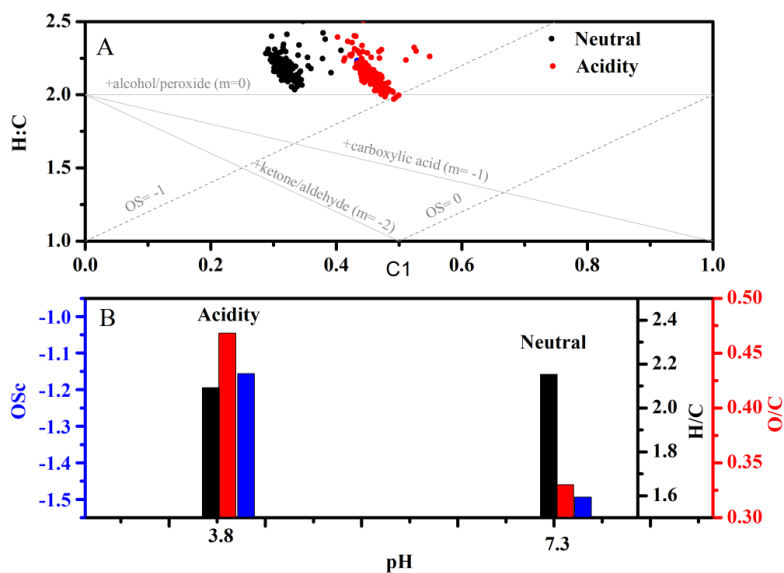
Figure 6. Van Krevelen diagrams of elemental ratios under different seed particle acidity (A); change in H/C ratio (black), O/C ratio (red), and OS_c (blue) with particle acidity (B).

Taken together, in the absence of seed particles, the homogeneous formation of more H_2SO_4 particles not only promoted the quick condensation of less- and more-oxygenated products and subsequent SOA formation via providing a greater surface area and volume, but enhanced the oligomerization process (Figure 7). In the presence of seed particles, the presence of more primary H_2SO_4 in seed particle enhanced EM uptake and functionalization process, but reduced SOA production due to the formation of surface H_2SO_4. This further indicated that the increase in primary and secondary H_2SO_4 particles could significantly affect SOA formation and composition.
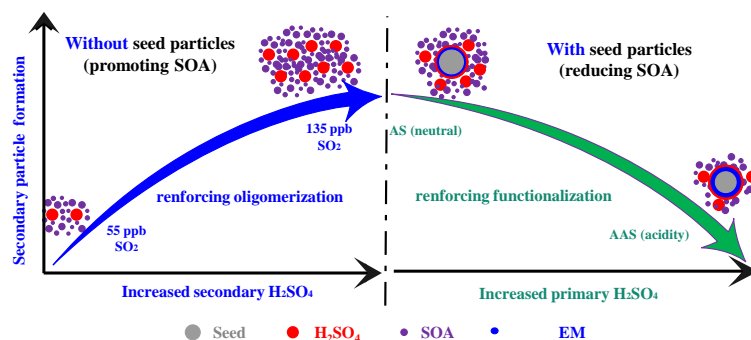
383

384   **Figure 7.** Proposed the role of H_2SO_4 formation on EM-derived SOA

385

386   **3.3. Reaction Mechanism of EM Ozonolysis**

387   In order to make clear the formation mechanism of EM-derived SOA, the

388   evolutions of some molecular ion peaks have been checked in detail. As shown in

389   Figure S15, the increase of their mass concentrations with reaction time indicated that

390   these molecular ions peaks with m/z 116, 130, 132, 140, 146, 148, 158, 162, 164, 176,

391   178, 180, 194, 196, and 212 should be the major ozonolysis products. Based on the

392   previously reported mechanism of alkene ozonolysis, the mechanism of EM ozonolysis

393   has been proposed in Scheme S1 (Jain et al., 2014;Vereecken and Francisco, 2012).

394   Briefly, oxidation of EM is initiated by addition of ozone across the double bound

395   resulting in a primary ozonide. The primary ozonide will produce two products

396   (formaldehyde and ketone ester) and two sCIs (sCI-1 and sCI-2). Based on the initial

397   carbonyl and sCI products (Scheme S1), it could be found that the saturated ketone ester

398   couldn't be further oxidized by O_3 and formaldehyde was the terminate products of sCI-

399   2 reaction. Thus, these major oxidation products observed in Figure S13 should come

400   from the further reaction of sCI-1.

401   Proposed reaction mechanism of sCI-1 was also shown in Scheme 1. These sCI-1 could

402   first convert to alkoxy radical (III) by losing OH group and O_2 addition. Then alkoxy

403   radical with an additional oxygen atom not only could further react with RO_2 to form

404   alcohols (V), but also react with HO_2 to form hydroperoxide product (IV). Moreover,

405   the intramolecular H-shift reaction may also compete with its bimolecular reaction with

406   HO$_2$ and other RO$_2$ radicals due to relatively weak C-H bonds in the molecule (Jokinen

407   et al., 2014;Crounse et al., 2013;Shu et al., 2018). Similarly, newly produced alkoxy

408   radical will continually and repeatedly react with HO$_2$, RO$_2$, and undergo its

409   intramolecular H-shift to form the higher oxidized alcohols, carbonyls, and

410   hydroperoxide product. The formation of these higher oxidized alcohols, carbonyls, and

411   hydroperoxide product might help to explain or give insight to the increased oxidation

412   state (OS$_c$) of the aerosol.

413

414

<figure>

(I) sCI
(III)
C$_5$H$_8$O$_5$ (m/z 148) (IV)
C$_5$H$_6$O$_4$ (m/z 130) (IV-1)
C$_5$H$_8$O$_4$ (m/z 132) (V)
C$_5$H$_8$O$_6$ (m/z 164) (VIII)
C$_5$H$_6$O$_5$ (m/z 146) (VIII-1)
C$_5$H$_6$O$_7$ (m/z 180) (IX)
C$_5$H$_6$O$_6$ (m/z 162) (VI)
C$_5$H$_6$O$_8$ (m/z 194) (VII)
C$_5$H$_8$O$_9$ (m/z 212) (X)
C$_5$H$_4$O$_7$ (m/z 176) (VII-1)
C$_5$H$_8$O$_8$ (m/z 196) (XI)
C$_5$H$_2$O$_6$ (m/z 158) (VII-2)
C$_5$H$_8$O$_8$ (m/z 178) (XI-1)

</figure>
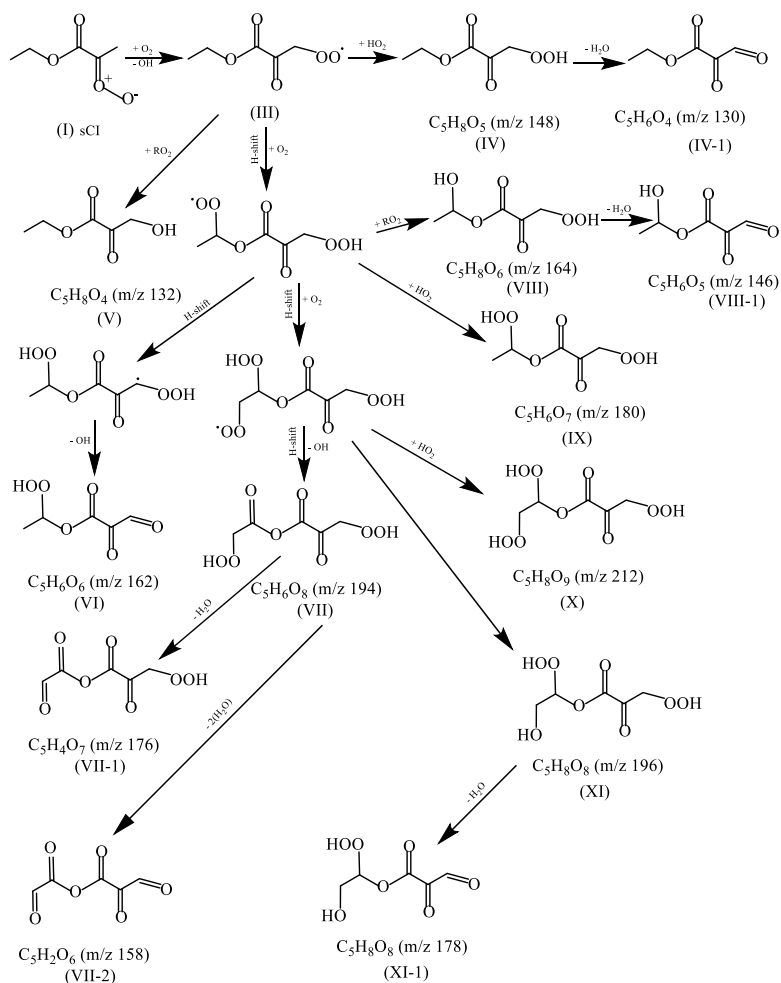
415   **Scheme 1.** Proposed mechanism for EM ozonolysis in the presence of AS particles

416

417   **4. Conclusion**

418   Some exposure measurement studies indicated that the concentration of ethyl

419   methacrylate was notably higher than other methacrylate in the salons working air. The

420   frequently exposure of methacrylate for a long time can trigger asthma or allergic

421   contact dermatitis. Thus, the wide variety of sources and high volatility and toxicity of

422   make EM a potential important source of environmental concern in the atmosphere.

423   In this work, we investigated and compared the formation of secondary particles

424   from EM ozonolysis under complex ambient condition. Results showed that a

425   substantial increase in secondary H_2SO_4 particles promoted SOA formation with

426   increasing SO_2. In contrast, the increase in primary H_2SO_4 proportion with seed acidity

427   enhanced EM uptake but reduced SOA formation. To clarify the underlying causes, we

428   analyzed the size distribution, chemical composition and evolution of SOA based on

429   PMF solutions and Van Krevelen diagrams. In the absence of seed particles, the

430   substantial increase in secondary H_2SO_4 particles with SO_2 provided greater surface

431   area and volume for further condensation of oxidation products. Moreover, enhanced

432   oligomerization functionalization of carbonyl species with increased particle acidity

433   also contributed to the increase in SOA in the absence of seed particles. However, in

434   the presence of seed particles, the increase of primary H_2SO_4 proportion in seed with

435   acidity enhanced more EM uptake, but the direct heterogeneous formation of H_2SO_4 on

436   the particle surface, differing from the condensation or nucleation of gas-phase H_2SO_4,

437   hampered the continuous heterogeneous ozonolysis of these adsorbed EM. Moreover,

438   even though increased particles acidity also caused chemical conversion of SOA via

439   functionalization, the contribution of the produced functionalized products to SOA

440   could be ignored due to the limited change in overall SOA formation. These results

441   indicated that the increase of primary and secondary H_2SO_4 particle has the different

442   effect on EM-derived SOA formation and its composition.

443   Taken together, our findings should not only help to clarify the SOA formation

444 mechanism of UVOEs ozonolysis in certain ambient environments particularly in
445 marine boundary layers and mid-continental regions, but should help to further
446 understand the complicated effects of increased H_2SO_4 components on SOA formation
447 and composition during haze pollution. In addition to EM, many other unsaturated
448 esters such as methyl methacrylate (MA), butyl methacrylate (BMA), and propyl
449 methacrylate (PMA) are also frequently measured in the real atmosphere (Blanco et al.,
450 2014;Ren et al., 2019). Thus more researches are needed to investigate the secondary
451 particles potential of these unsaturated esters, especially under complex ambient
452 conditions, which will help to further effectively evaluate the potential contribution of
453 their atmospheric oxidation process to secondary particle formation.
454

455 **Corresponding Author and Author Contributions**

456 * Phone: (+86)-010-62849508;
457 E-mail: qxma @rcees.ac.cn.
458 E-mail: bwchu @rcees.ac.cn.
459 PZ and TC designed and conducted this experiment, TC helped to analyze experimental
460 data. JL, XG, and WS gave assistance in measurements. HH, QM and BC discussed the
461 data results. PZ wrote the paper with input from all coauthors. All authors contributed
462 to the final paper.
463

464 **Notes**

465 The authors declare no competing financial interests.
466

467 **Acknowledgments**

468 This work was financially supported by the National Natural Science Foundation of
469 China (41605100, 41705134, 21876185, 91744205, and 41877304).
470

471 **References**

472 Arey, J., Winer, A.M., Atkinson, R., Aschmann, S.M., Long, W.D., Morrison, C.L.: The emission of (Z)-
473 3-hexen-1-ol,(Z)-3-hexenylacetate and other oxygenated hydrocarbons from agricultural plant species,

474   Atmos. Environ. Part A. General Topics., 25, 1063-1075, https://doi.org/10.1016/0960-1686(91)90148-
475   Z,1991.

476   Bernard, F., Eyglunent, G., Daele, V., Mellouki, A.: Kinetics and products of gas-phase reactions of ozone
477   with methyl methacrylate, methyl acrylate, and ethyl acrylate, J. Phys.Chem. A., 114, 8376-8383,
478   https://doi.org/10.1021/jp104451v , 2010.

479   Blanco, M.a.B., Bejan, I., Barnes, I., Wiesen, P., Teruel, M.A.: FTIR product distribution study of the Cl
480   and OH initiated degradation of methyl acrylate at atmospheric pressure, Environ. Sci. Tech., 44, 7031-
481   7036, https://doi.org/10.1021/es101831r, 2010.

482   Blanco, M.B., Bejan, I., Barnes, I., Wiesen, P., Teruel, M.A.: Products and Mechanism of the Reactions
483   of OH Radicals and Cl Atoms with Methyl Methacrylate (CH$_2$=C (CH$_3$) C (O) OCH$_3$) in the Presence of
484   NOx, Environ. Sci. Tech., 48, 1692-1699, https://doi.org/10.1021/es404771d, 2014.

485   Chen, Q., Liu, Y., Donahue, N.M., Shilling, J.E., Martin, S.T.: Particle-phase chemistry of secondary
486   organic material: modeled compared to measured O: C and H: C elemental ratios provide constraints,
487   Environ. Sci. Tech., 45, 4763-4770, https://doi.org/10.1021/es104398s, 2011.

488   Chen, T., Liu, Y., Ma, Q., Chu, B., Zhang, P., Liu, C., Liu, J., He, H.: Significant source of secondary
489   aerosol: formation from gasoline evaporative emissions in the presence of SO$_2$ and NH$_3$, Atmos. Chem.
490   Phys., 19, 8063-8081, https://doi.org/10.5194/acp-19-8063-2019, , 2019.

491   Chu, B., Zhang, X., Liu, Y., He, H., Sun, Y., Jiang, J., Li, J., Hao, J.: Synergetic formation of secondary
492   inorganic and organic aerosol: effect of SO$_2$ and NH$_3$ on particle formation and growth, Atmos. Chem.
493   Phys., 16, 14219-14230, https://doi:10.5194/acp-16-14219-2016, 2016.

494   Colomer, J.P., Blanco, M.B., Peñéñory, A.B., Barnes, I., Wiesen, P., Teruel, M.A.: FTIR gas-phase kinetic
495   study on the reactions of OH radicals and Cl atoms with unsaturated esters: Methyl-3, 3-dimethyl
496   acrylate,(E)-ethyl   tiglate   and   methyl-3-butenoate,   Atmos.   Environ.,   79,   546-552,
497   https://doi.org/10.1016/j.atmosenv.2013.07.009,2013.

498   Crounse, J.D., Nielsen, L.B., Jørgensen, S., Kjaergaard, H.G., Wennberg, P.O.: Autoxidation of organic
499   compounds   in   the   atmosphere,   J.   Phys.   Chem.   Lett.,   4,   3513-3520,
500   https://doi.org/10.1021/jz4019207,2013.

501   Darer, A.I., Cole-Filipiak, N.C., O'Connor, A.E., Elrod, M.J.: Formation and stability of atmospherically
502   relevant isoprene-derived organosulfates and organonitrates, Environ. Sci. Tech., 45, 1895-1902,
503   https://doi.org/10.1021/es103797z, 2011.

504   Drewnick, F., Hings, S.S., DeCarlo, P., Jayne, J.T., Gonin, M., Fuhrer, K., Weimer, S., Jimenez, J.L.,
505   Demerjian, K.L., Borrmann, S.: A new time-of-flight aerosol mass spectrometer (TOF-AMS)—
506   Instrument   description   and   first   field   deployment,   Aerosol.   Sci.   Tech.,   39,   637-658,
507   https://doi.org/10.1080/02786820500182040, 2005.

508   Eddingsaas, N., Loza, C., Yee, L., Chan, M., Schilling, K., Chhabra, P., Seinfeld, J., Wennberg, P.: α-
509   pinene photooxidation under controlled chemical conditions–Part 2: SOA yield and composition in low-
510   and high-NOx environments, Atmos. Chem. Phys., 12, 7413-7427, https:// doi:10.5194/acp-12-6489-
511   2012, 2012.

512   Friedman, B., Brophy, P., Brune, W.H., Farmer, D.K.: Anthropogenic sulfur perturbations on biogenic
513   oxidation: SO$_2$ additions impact gas-phase OH oxidation products of α- and β-pinene, Environ. Sci. Tech.,
514   50, 1269-1279, https://doi.org/10.1021/acs.est.5b05010, 2016.

515   Gordon, T., Presto, A., May, A., Nguyen, N., Lipsky, E., Donahue, N., Gutierrez, A., Zhang, M., Maddox,
516   C., Rieger, P.: Secondary organic aerosol formation exceeds primary particulate matter emissions for
517   light-duty gasoline vehicles, Atmos. Chem. Phys., 14, 4661-4678, https://doi:10.5194/acp-14-4661-201,

518   2014.

519   Hamilton, J., Lewis, A., Carey, T., Wenger, J., Borrás i Garcia, E., Munoz, A.: Reactive oxidation

520   products promote secondary organic aerosol formation from green leaf volatiles, Atmos. Chem. Phys. 9.,

521   3815-3823, https://doi.org/10.5194/acp-9-3815-2009, 2009.

522   Han, Y., Stroud, C.A., Liggio, J., Li, S.-M.: The effect of particle acidity on secondary organic aerosol

523   formation from α-pinene photooxidation under atmospherically relevant conditions, Atmos. Chem. Phys.,

524   16, 13929-13944, http://doi:10.5194/acp-16-13929-2016, 2016.

525   Harvey, R.M., Bateman, A.P., Jain, S., Li, Y.J., Martin, S., Petrucci, G.A.: Optical properties of secondary

526   organic aerosol from cis-3-hexenol and cis-3-hexenyl acetate: effect of chemical composition, humidity,

527   and phase, Environ. Sci. Tech., 50, 4997-5006, https://doi.org/10.1021/acs.est.6b00625, 2016.

528   Heald, C., Kroll, J., Jimenez, J., Docherty, K., DeCarlo, P., Aiken, A., Chen, Q., Martin, S., Farmer, D.,

529   Artaxo, P.: A simplified description of the evolution of organic aerosol composition in the atmosphere,

530   Geophys. Res. Lett., 37, (8), https://doi.org/10.1029/2010GL042737, 2010.

531   Hearn, J.D., Lovett, A.J., Smith, G.D.: Ozonolysis of oleic acid particles: evidence for a surface reaction

532   and secondary reactions involving Criegee intermediates, Phys. Chem. Chem. Phys., 7, 501-511,

533   https://doi.org/10.1039/B414472D, 2005.

534   Hennigan, C., Izumi, J., Sullivan, A., Weber, R., Nenes, A.: A critical evaluation of proxy methods used

535   to estimate the acidity of atmospheric particles,. Atmos. Chem. Phys., 15, 2775-2790, doi:10.5194/acp-

536   15-2775-2015, 2015.

537   Henriks-Eckerman, M.-L., Korva, M.: Exposure to airborne methacrylates in nail salons, J. Occup.

538   Environ. Hyg., 9, D146-D150, https://doi.org/10.1080/15459624.2012.696023, 2012.

539   Jain, S., Zahardis, J., Petrucci, G.A.: Soft ionization chemical analysis of secondary organic aerosol from

540   green   leaf   volatiles   emitted   by   turf   grass,   Environ.   Sci.   Tech.,   48,   4835-4843,

541   https://doi.org/10.1021/es405355d, 2014.

542   Jokinen, T., Sipilä, M., Richters, S., Kerminen, V.M., Paasonen, P., Stratmann, F., Worsnop, D., Kulmala,

543   M., Ehn, M., Herrmann, H.: Rapid autoxidation forms highly oxidized RO_2 radicals in the atmosphere,

544   Angew. Chem. Int. Ed., 53, 14596-14600, https://doi.org/10.1002/anie.201408566, 2014.

545   König, G., Brunda, M., Puxbaum, H., Hewitt, C.N., Duckham, S.C., Rudolph, J.,: Relative contribution

546   of oxygenated hydrocarbons to the total biogenic VOC emissions of selected mid-European agricultural

547   and natural plant species, Atmos. Environ., 29, 861-874, https://doi.org/10.1016/1352-2310(95)00026-

548   U, 1995.

549   Kristensen, K., Cui, T., Zhang, H., Gold, A., Glasius, M., Surratt, J.: Dimers in α-pinene secondary

550   organic aerosol: effect of hydroxyl radical, ozone, relative humidity and aerosol acidity, Atmos. Chem.

551   Phys., 14, 4201-4218, http://doi:10.5194/acp-14-4201-2014, 2014.

552   Lambe, A., Onasch, T., Massoli, P., Croasdale, D., Wright, J., Ahern, A., Williams, L., Worsnop, D.,

553   Brune, W.H., Davidovits, P.: Laboratory studies of the chemical composition and cloud condensation

554   nuclei (CCN) activity of secondary organic aerosol (SOA) and oxidized primary organic aerosol (OPOA),

555   Atmos. Chem. Phys., 11, 8913-8928, http://doi:10.5194/acp-11-8913-2011, 2011.

556   Lambe, A.T., Onasch, T.B., Croasdale, D.R., Wright, J.P., Martin, A.T., Franklin, J.P., Massoli, P., Kroll,

557   J.H., Canagaratna, M.R., Brune, W.H.:Transitions from functionalization to fragmentation reactions of

558   laboratory secondary organic aerosol (SOA) generated from the OH oxidation of alkane precursors,

559   Environ. Sci. Tech., 46, 5430-5437, https://doi.org/10.1021/es300274t, 2012.

560   Li, K., Liggio, J., Lee, P., Han, C., Liu, Q., Li, S.-M.: Secondary organic aerosol formation from α-pinene,

561   alkanes, and oil-sands-related precursors in a new oxidation flow reactor, Atmos. Chem. Phys., 19, 9715-

562   9731, https://doi.org/10.5194/acp-19-9715-2019, 2019.

563   Lin, Y.-H., Knipping, E., Edgerton, E., Shaw, S., Surratt, J.: Investigating the influences of SO$_2$ and NH$_3$

564   levels on isoprene-derived secondary organic aerosol formation using conditional sampling approaches,.

565   Atmos. Chem. Phys., 13, 8457-8470, https://doi.org/10.5194/acp-13-8457-2013, 2013.

566   Lin, Y.-H., Zhang, Z., Docherty, K.S., Zhang, H., Budisulistiorini, S.H., Rubitschun, C.L., Shaw, S.L.,

567   Knipping, E.M., Edgerton, E.S., Kleindienst, T.E.: Isoprene epoxydiols as precursors to secondary

568   organic aerosol formation: acid-catalyzed reactive uptake studies with authentic compounds, Environ.

569   Sci. Tech., 46, 250-258, https://doi.org/10.1021/es202554c, 2011.

570   Liu, C., Chen, T., Liu, Y., Liu, J., He, H., Zhang, P.: Enhancement of secondary organic aerosol formation

571   and its oxidation state by SO$_2$ during photooxidation of 2-methoxyphenol, Atmos. Chem. Phys., 19,

572   2687-2700, https://doi.org/10.5194/acp-19-2687-2019, 2019a.

573   Liu, C., Liu, Y., Chen, T., Liu, J., He, H.: Rate constant and secondary organic aerosol formation from

574   the gas-phase reaction of eugenol with hydroxyl radicals, Atmos. Chem. Phys., 19, 2001-2013.

575   http://doi:10.5194/acp-19-2001-2019, 2019b.

576   Liu, S., Jia, L., Xu, Y., Tsona, N.T., Ge, S., Du, L.: Photooxidation of cyclohexene in the presence of SO$_2$:

577   SOA   yield   and   chemical   composition,   Atmos.   Chem.   Phys.,   17,   13329-13343,

578   https://doi.org/10.5194/acp-17-13329-2017, 2017.

579   Liu, S., Jiang, X., Tsona, N.T., Lv, C., Du, L.: Effects of NOx, SO$_2$ and RH on the SOA formation from

580   cyclohexene   photooxidation,   Chemosphere.,   216,   794-804,

581   https://doi.org/10.1016/j.chemosphere.2018.10.180, 2019.

582   Newland, M.J., Rickard, A.R., Alam, M.S., Vereecken, L., Munoz, A., Rodenas, M., Bloss, W.J., :

583   Kinetics of stabilised Criegee intermediates derived from alkene ozonolysis: reactions with SO$_2$, H$_2$O

584   and decomposition under boundary layer conditions, Phys. Chem. Chem. Phys., 17, 4076-4088,

585   http://doi:10.1039/c4cp04186k, 2015a.

586   Newland, M.J., Rickard, A.R., Vereecken, L., Munoz, A., Rodenas, M., Bloss, W.J.: Atmospheric

587   isoprene ozonolysis: impacts of stabilised Criegee intermediate reactions with SO$_2$, H$_2$O and dimethyl

588   sulfide, Atmos. Chem. Phys., 15, 9521-9536, http:// doi:10.5194/acp-15-9521-2015, 2015b.

589   Ng, N., Canagaratna, M., Jimenez, J., Chhabra, P., Seinfeld, J., Worsnop, D.: Changes in organic aerosol

590   composition with aging inferred from aerosol mass spectra, Atmos. Chem. Phys., 11, 6465-6474, http://

591   doi:10.5194/acp-11-6465-2011, 2011.

592   Offenberg, J.H., Lewandowski, M., Edney, E.O., Kleindienst, T.E., Jaoui, M.: Influence of aerosol acidity

593   on the formation of secondary organic aerosol from biogenic precursor hydrocarbons. Environ. Sci. Tech.

594   43, 7742-7747, http:// doi:10.1021/es901538e, 2009.

595   Pankow, J.F., Luo, W., Bender, D.A., Isabelle, L.M., Hollingsworth, J.S., Chen, C., Asher, W.E., Zogorski,

596   J.S.: Concentrations and co-occurrence correlations of 88 volatile organic compounds (VOCs) in the

597   ambient air of 13 semi-rural to urban locations in the United States, Atmos. Environ., 37, 5023-5046,

598   https://doi.org/10.1016/j.atmosenv.2003.08.006, 2003.

599   Peng, X., Vasilakos, P., Nenes, A., Shi, G., Qian, Y., Shi, X., Xiao, Z., Chen, K., Feng, Y., Russell, A.G.:

600   Detailed Analysis of Estimated pH, Activity Coefficients, and Ion Concentrations between the Three

601   Aerosol   Thermodynamic   Models,   Environ.   Sci.   Tech.,   53,   8903-8913,

602   https://doi.org/10.1021/acs.est.9b00181, 2019.

603   Ren, Y., Cai, M., Daële, V., Mellouki, A.: Rate coefficients for the reactions of OH radical and ozone

604   with   a   series   of   unsaturated   esters,   Atmos.   Environ.,   200,   243-253,

605   https://doi.org/10.1016/j.atmosenv.2018.12.017, 2019.

606   Riva, M., Bell, D.M., Hansen, A.-M.K., Drozd, G.T., Zhang, Z., Gold, A., Imre, D., Surratt, J.D., Glasius,
607   M., Zelenyuk, A.: Effect of organic coatings, humidity and aerosol acidity on multiphase chemistry of
608   isoprene epoxydiols, Environ. Sci. Tech., 50, 5580-5588, https://doi.org/10.1021/acs.est.5b06050, 2016.
609   Rivela, C.B., Blanco, M.B., Teruel, M.A.: Atmospheric degradation of industrial fluorinated acrylates
610   and methacrylates with Cl atoms at atmospheric pressure and 298 K, Atmos. Environ., 178, 206-213,
611   https://doi.org/10.1016/j.atmosenv.2018.01.055, 2018.
612   Sadezky, A., Chaimbault, P., Mellouki, A., Römpp, A., Winterhalter, R., Bras, G.L., Moortgat, G.:
613   Formation of secondary organic aerosol and oligomers from the ozonolysis of enol ethers, Atmos. Chem.
614   Phys., 6, 5009-5024, http://doi:10.5194/acp-6-5009-2006, 2006.
615   Sadezky, A., Winterhalter, R., Kanawati, B., Römpp, A., Spengler, B., Mellouki, A., Bras, G.L.,
616   Chaimbault, P., Moortgat, G.: Oligomer formation during gas-phase ozonolysis of small alkenes and enol
617   ethers: new evidence for the central role of the Criegee Intermediate as oligomer chain unit, Atmos. Chem.
618   Phys., 8, 2667-2699, https://doi.org/10.5194/acp-8-2667-2008, 2008.
619   Salgado, M.S., Gallego-Iniesta, M.P., Martín, M.P., Tapia, A., Cabañas, B.: Night-time atmospheric
620   chemistry of methacrylates, Environ. Sci. Pollut. R., 18, 940-948, http://doi:10.1007/s11356-011-0448-
621   x, 2011.
622   Shu, Y., Ji, J., Xu, Y., Deng, J., Huang, H., He, M., Leung, D.Y.C., Wu, M., Liu, S., Liu, S., Liu, G., Xie,
623   R., Feng, Q., Zhan, Y., Fang, R., Ye, X.: Promotional role of Mn doping on catalytic oxidation of VOCs
624   over mesoporous TiO_2 under vacuum ultraviolet (VUV) irradiation, Appl. Catal. B-Environ., 220, 78-87,
625   https://doi.org/10.1016/j.apcatb.2017.08.019, 2018.
626   Srivastava,   S.:Co-polymerization   of   acrylates,   *De*s.   Monomers.   Polym.,   12,   1-18,
627   https://doi.org/10.1163/156855508X391103, 2009.
628   Sun, Y., Zhang, Q., Hu, J., Chen, J., Wang, W.: Theoretical study for OH radical-initiated atmospheric
629   oxidation of ethyl acrylate, Chemosphere., 119, 626-633, http:// doi:10.1016/j.chemosphere.2014.07.056,
630   2015.
631   Surratt, J.D., Chan, A.W., Eddingsaas, N.C., Chan, M., Loza, C.L., Kwan, A.J., Hersey, S.P., Flagan, R.C.,
632   Wennberg, P.O., Seinfeld, J.H.: Reactive intermediates revealed in secondary organic aerosol formation
633   from isoprene, P. Natl. Acad. Sci., 107, 6640-6645, https://doi.org/10.1073/pnas.0911114107, 2010.
634   Taccone, R.A., Moreno, A., Colmenar, I., Salgado, S., Martín, M.P., Cabañas, B.: Kinetic study of the
635   OH, NO_3 radicals and Cl atom initiated atmospheric photo-oxidation of iso-propenyl methyl ether, Atmos.
636   Environ., 127, 80-89, http://doi:10.1016/j.atmosenv.2015.12.033, 2016.
637   Teruel, M.A., López, R.S.P., Barnes, I., Blanco, M.B.: Night-time atmospheric degradation of a series of
638   butyl   methacrylates,   Chemical   Physics   Letters.,   664,   205-212,
639   https://doi.org/10.1016/j.cplett.2016.09.040, 2016.
640   Ulbrich, I., Canagaratna, M., Zhang, Q., Worsnop, D., Jimenez, J.: Interpretation of organic components
641   from Positive Matrix Factorization of aerosol mass spectrometric data, Atmos. Chem., Phys. 9, 2891-
642   2918, http://doi:10.5194/acp-9-2891-2009, 2009.
643   Vereecken, L., Francisco, J.S.: Theoretical studies of atmospheric reaction mechanisms in the
644   troposphere, Chem. Soc. Rev., 41, 6259-6293, http:// doi:10.1039/c2cs35070j, 2012.
645   Wang, K., Ge, M., & Wang, W.: Kinetics of the gas-phase reactions of NO_3 radicals with ethyl acrylate,
646   n-butyl acrylate, methyl methacrylate and ethyl methacrylate, Atmos. Environ., 44(15), 1847–1850.
647   http://doi:10.1016/j.atmosenv.2010.02.039, 2010.
648   Wang, M., Yao, L., Zheng, J., Wang, X., Chen, J., Yang, X., Worsnop, D.R., Donahue, N.M., Wang, L.:
649   Reactions of atmospheric particulate stabilized Criegee intermediates lead to high-molecular-weight

650   aerosol components, Environ. Sci. Tech., 50, 5702-5710, https://doi.org/10.1021/acs.est.6b02114, 2016.

651   Wong, J.P., Lee, A.K., Abbatt, J.P.: Impacts of sulfate seed acidity and water content on isoprene

652   secondary   organic   aerosol   formation,   Environ.   Sci.   Tech.,   49,   13215-13221,

653   https://doi.org/10.1021/acs.est.5b02686, 2015.

654   Zhang, P., Chen, T., Liu, J., Liu, C., Ma, J., Ma, Q., Chu, B., He, H.: Impacts of SO_2, Relative Humidity,

655   and Seed Acidity on Secondary Organic Aerosol Formation in the Ozonolysis of Butyl Vinyl Ether,

656   Environ. Sci. Tech., 53, 8845-8853, https://doi.org/10.1021/acs.est.9b02702, 2019.

657   Zhang, Q., Alfarra, M.R., Worsnop, D.R., Allan, J.D., Coe, H., Canagaratna, M.R., Jimenez, J.L.:

658   Deconvolution and quantification of hydrocarbon-like and oxygenated organic aerosols based on aerosol

659   mass spectrometry, Environ. Sci. Tech., 39, 4938-4952, https://doi.org/10.1021/es048568l, 2005.

660   Zhang, Q., Jimenez, J.L., Canagaratna, M.R., Ulbrich, I.M., Ng, N.L., Worsnop, D.R., Sun, Y.:

661   Understanding atmospheric organic aerosols via factor analysis of aerosol mass spectrometry: a review,

662   Anal. Bioanal. Chem., 401, 3045-3067, http://doi:10.1007/s00216-011-5355-y, 2011.

663   Zhang, X., Cappa, C.D., Jathar, S.H., Mcvay, R.C., Ensberg, J.J., Kleeman, M.J., Seinfeld, J.H.: Influence

664   of vapor wall loss in laboratory chambers on yields of secondary organic aerosol, P. Natl. Acad. Sci., 111,

665   5802-5807, https://doi.org/10.1073/pnas.1404727111,2014.

666   Zhao, D., Schmitt, S.H., Wang, M., Acir, I.-H., Tillmann, R., Tan, Z., Novelli, A., Fuchs, H., Pullinen, I.,

667   Wegener, R.: Effects of NOx and SO_2 on the secondary organic aerosol formation from photooxidation

668   of α-pinene and limonene, Atmos. Chem. Phys., 18, 1611-1628, http://dx.doi.org/10.5194/acp-18-1611-

669   2018, 2018.

670

671

672